USGS
science for a changing world

Prepared in cooperation with the Mason Conservation District

Bedload and Suspended-Sediment Transport in Lower Vance Creek, Western Washington, Water Years 2019–20

Scientific Investigations Report 2022–5019

U.S. Department of the Interior
U.S. Geological Survey

Front cover. Streamgage and bedload sampling from the Skokomish Valley Road bridge over Vance Creek, December 13, 2018. Photo by Kristin Jaeger, U.S. Geological Survey.

Back cover. U.S. Geological Survey hydrologist retrieving a bedload sample using Toutle River II bedload sampler, Vance Creek, December 13, 2018. Photo by Kristin Jaeger, U.S. Geological Survey.

Bedload and Suspended-Sediment Transport in Lower Vance Creek, Western Washington, Water Years 2019–20

By Scott W. Anderson

Prepared in cooperation with the Mason Conservation District

Scientific Investigations Report 2022–5019

U.S. Geological Survey, Reston, Virginia: 2022

Suggested citation:
Anderson, S.W., 2022, Bedload and suspended-sediment transport in lower Vance Creek, western Washington, water years 2019–20: U.S. Geological Survey Scientific Investigations Report 2022–5019, 25 p., https://doi.org/10.3133/sir20225019.

ISSN 2328-0328 (online)

Acknowledgments

Chris Curran, Stephen Sissel, and Dan Restivo of the U.S. Geological Survey all provided substantial help in coordinating sampling trips and equipment, as well as leading discharge and suspended-sediment sampling efforts in the field. Kevin Linn and Mark Mastin of the U.S. Geological Survey were instrumental in discussions regarding discharge and rating curves at various streamgage sites. Kristin Jaeger, Andrew Gendaszek, Allison Tecca, Alex Headman, Norm Peterson, Michelle Fox, Tanner Saarela, and Vince Walzem of the U.S. Geological Survey all provided much appreciated help with bedload sampling. Brian Collins of the University of Washington provided hard copies of the 1994 Simons and Associates data.

Contents

Figures

Tables

Conversion Factors

U.S. customary units to International System of Units

Multiply	By	To obtain
	Length	
inch (in.)	25.4	millimeter (mm)
foot (ft)	0.3048	meter (m)
mile (mi)	1.609	kilometer (km)
	Area	
square mile (mi^2)	2.590	square kilometer (km^2)
	Flow rate	
cubic foot per second (ft^3/s)	0.02832	cubic meter per second (m^3/s)
	Mass	
pound, avoirdupois (lb)	0.4536	kilogram (kg)
ton, short (2,000 lb)	0.9072	metric ton (t)

International System of Units to U.S. customary units

Multiply	By	To obtain
	Length	
millimeter (mm)	0.03937	inch (in.)
	Mass	
kilogram (kg)	2.205	pound avoirdupois (lb)
	Density	
milligrams per liter (mg/L)	0.000062	pound per cubic foot (lb/ft^3)

Datum

Horizontal coordinate information is referenced to the North American Datum of 1983 (NAD 83).

Supplemental Information

Concentrations of suspended sediments and bedload are given in milligrams per liter (mg/L).

Abbreviations

EDI	equal-discharge increment
EWI	equal-width increment
NWIS	National Water Information System
OLS	ordinary least squares regression
PDT	Pacific Daylight Time
POR	period of record
SSC	suspended-sediment concentration
SSL	suspended-sediment load
USGS	U.S. Geological Survey
USGS–CVO	U.S. Geological Survey's–Cascades Volcano Observatory
USGS–WAWSC	U.S. Geological Survey's–Washington Water Science Center

Bedload and Suspended-Sediment Transport in Lower Vance Creek, Western Washington, Water Years 2019–20

By Scott W. Anderson

Abstract

Vance Creek drains a 24 square mile area of the Olympic Mountains in western Washington. The lower 4 miles of the creek often go dry in discontinuous patches during the summer, limiting salmon rearing success. To better understand sediment transport dynamics in the creek and aid in potential restoration design, bedload and suspended-sediment concentration samples were collected for water years 2019–20 at a site about 2 miles upstream from the creek's confluence with the South Fork Skokomish River.

Fifty bedload samples and 7 suspended-sediment concentration samples were collected over 7 sampling days. These samples were used to develop rating curves relating bedload flux or suspended-sediment concentration to discharge. Mean annual bedload flux was estimated to be 12,200 ± 2,300 tons per year for water years 1930–2020 period of record, based on application of the derived bedload rating curve to an extrapolated daily discharge record. The mean annual suspended-sediment load over the same period was estimated to be 9,000 tons per year with large, but unquantified, uncertainty. Bedload material was predominantly gravel from 0.08 to 2.5 inches (2 to 64 millimeters) in diameter. At the highest sampled discharges, approximately equivalent to a 50 percent annual exceedance probability (2-year peak-flow event), the bedload grain-size distribution was similar to that of the local channel bed. Bedload grain-size distributions generally coarsened as discharge increased. The suspended-sediment load was consistently one-half sand and one-half silt and clay, regardless of discharge. Bedload constituted about 60 percent of the total sediment flux (bedload plus suspended load). This is near the upper limit of values observed in a global compilation of long-term load partitioning data.

Sediment transport at the Vance Creek sampling site was compared with sediment-transport data from five other watersheds in the region. To facilitate comparisons, mean annual loads were divided by mean annual runoff volume to obtain an effective average sediment concentration. This normalization accounts for differences in both drainage area and mean runoff depth between the comparison watersheds. At the three comparison watershed sites with relatively complete sediment-transport data, mean bedload concentrations ranged from 44 to 109 milligrams per liter (mg/L) and mean suspended-sediment concentrations ranged from 139 to 374 mg/L; bedload constituted 21 to 29 percent of the total sediment load. The mean bedload concentration at the Vance Creek sampling site (69 mg/L) fell in the middle of the range observed in comparison watersheds, whereas the mean suspended-sediment concentration (50 mg/L) was markedly lower. Bedload samples at the Vance Creek sampling site also were generally less sand rich (sample-average sand fraction was 13 percent at Vance Creek versus 20 to 37 percent for comparison waters). Bedload transport rates at the Vance Creek sampling site appear relatively average for the region, given the drainage basin area and average runoff. In contrast, the supply and transport of finer material, both in the suspended load and the sand fraction of the bedload, are relatively low.

Introduction

Vance Creek is a gravel bedded river draining 24 square miles (mi^2) in the southeastern corner of the Olympic Mountains, western Washington (fig. 1). The lower 4 miles of the creek often go dry in discontinuous patches during the summer (Bountry and Godaire, 2011), limiting the potential rearing success of a variety of salmonid species that make use of the creek. This issue has prompted a discussion of potential efforts that might improve low-flow connectivity and habitat. However, the selection and design of such efforts is currently hampered by a limited knowledge of sediment transport conditions, and particularly bedload transport conditions, in the river system.

To address this gap in knowledge, the U.S. Geological Survey, in collaboration with the Mason Conservation District, conducted a campaign of collecting bedload and suspended-sediment samples in Vance Creek for water years 2019–20. The collected sediment samples were used to characterize the magnitude and grain-size distribution of the creek's sediment flux and, coupled with discharge records from a co-located streamgage, used to estimate annual sediment loads.

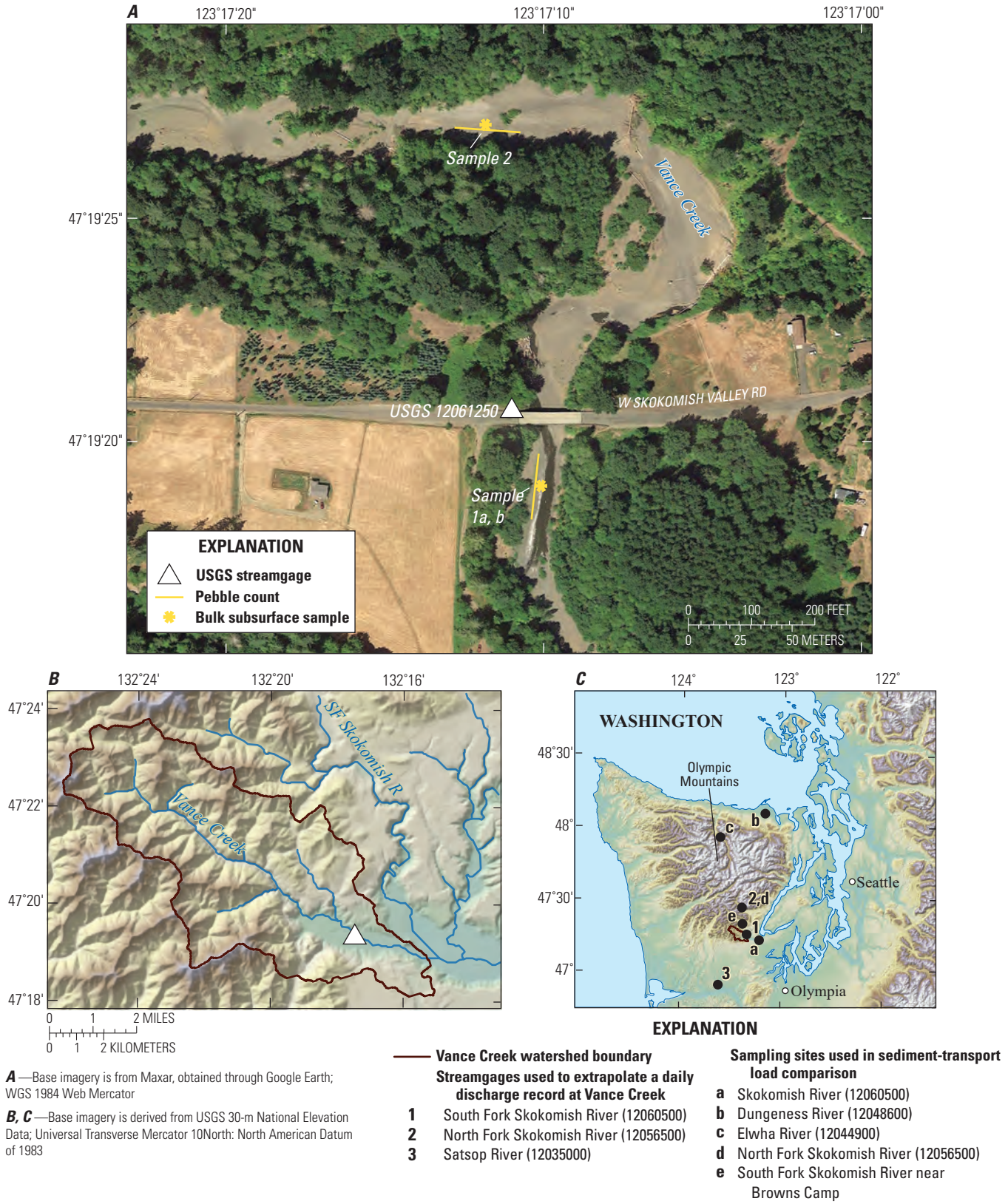

A —Base imagery is from Maxar, obtained through Google Earth; WGS 1984 Web Mercator

B, C —Base imagery is derived from USGS 30-m National Elevation Data; Universal Transverse Mercator 10North: North American Datum of 1983

Figure 1. Site maps showing Vance Creek, western Washington. *A*, aerial image of mostly dry Vance Creek in the vicinity of the sampling site. *B*, the Vance Creek drainage basin with sampling site marked with a white triangle. *C*, Vance Creek drainage basin in regional context.

Study Site

Vance Creek is a mid-sized tributary of the South Fork Skokomish River (fig. 1*B*). The upper drainage basin is composed of steep, forested terrain predominantly underlain by Eocene basalt and flow breccias (Washington State Department of Natural Resources, 2016). In the upper drainage basin, both Vance Creek and its tributaries run in narrow, tightly confined channels bounded by steep and heavily forested hillslopes. About 4 miles upstream from its confluence with the South Fork Skokomish River, Vance Creek emerges onto a broad lowland valley, transitioning to a meandering river with extensive gravel deposits and flanked by a mix of floodplain and terrace surfaces. This broad valley is mantled with relatively young alluvium and bounded by a mix of glacial and glaciofluvial deposits (Washington State Department of Natural Resources, 2016; Bountry and Godaire, 2011).

All discharge monitoring and sediment sampling occurred around the Skokomish Valley Road bridge, located approximately 1.8 river miles upstream from the South Fork Skokomish River confluence (figs. 1–2). The river immediately upstream from the bridge makes a series of sharp bends, which have been migrating relatively rapidly in recent decades, but then runs straight under the bridge and for several hundred yards downstream. A U.S. Geological Survey (USGS) streamgage (Vance Creek above Kirkland Creek, near Potlatch, Washington, USGS 12061250) was established at this site on September 28, 2018, providing 15-minute stage and discharge records for the period of this study.

Purpose and Scope

The purpose of this study is to characterize bedload and suspended-sediment transport rates and annual fluxes in Vance Creek, western Washington. These data inform resource managers seeking to both reduce local flood hazards and improve the aquatic ecosystem and rearing success of various salmonid species that make use of the creek.

The goals of the study were to (1) collect discrete measurements of bedload-transport rates and suspended-sediment concentrations, (2) develop relations between discharge and bedload and between discharge and suspended-sediment concentrations, (3) provide estimates of annual loads, yields, concentrations, and grain-size distributions for bedload and suspended sediment for Vance Creek, and (4) compare sediment-transport conditions in Vance Creek relative to nearby rivers in the region.

Estimating Long-Term Discharge Records

To extend the available discharge record beyond the 2 years provided by the Vance Creek streamgage (12061250), a daily mean discharge record for Vance Creek from water years 1930 to 2020 was estimated based on correlations with long-term streamgages on the South Fork Skokomish River (USGS 12060500; period of record (POR) 1931–84, 1995–present [2020]), the North Fork Skokomish River (USGS 12056500, POR 1924–present [2020]) and the Satsop River (USGS 12035000; POR 1929–present [2020]). Locations of these streamgages are shown in figure 1*C*.

Cross-correlation of 15-minute discharge records was first used to identify lag times between Vance Creek and the other three streamgages. On average, discharge in Vance Creek led the South Fork Skokomish River by 1 hour, lagged the North Fork Skokomish River by 1.5 hours, and led the Satsop River by 5.5 hours. The 15-minute discharge records for the South Fork Skokomish River, North Fork Skokomish River, and the Satsop River streamgages were offset accordingly and then summarized to daily mean values. These lag-offset daily mean discharge records were then used to develop correlations with daily mean discharge in Vance Creek.

Relations between Vance Creek daily mean discharge and the various streamgages were described using locally estimated scatterplot smoothing (LOESS; Cleveland and Devlin, 1988) curve fits (fig. 3). To extrapolate beyond the range of discharges encountered over the 2-year monitoring period, LOESS curves were extended based on a linear extrapolation of the upper end of the fitted curve, defined as days when Vance Creek daily mean discharge exceeded 1,000 cubic feet per second (ft^3/s). The estimated discharges at Vance Creek from the three reference streamgages were averaged to create a final daily discharge record starting in water year 1930 and extending through water year 2020.

Figure 2. Images showing the sampling site, Vance Creek, western Washington. Photographs are from the Skokomish Valley Road bridge across Vance Creek (fig. 1*A*). *A*, photograph looking downstream during summer dry conditions, September 6, 2018. *B*, same perspective as *A*, but at 2,700 cubic feet per second, January 23, 2020. *C*, Toutle River II bedload sampler, January 23, 2020. *D*, D-74 suspended-sediment sampler, February 1, 2020. [Photograph in *A*, by Kris Jaeger, U.S. Geological Survey. Photographs in *B*, *C*, and *D* by Scott Anderson, U.S. Geological Survey].

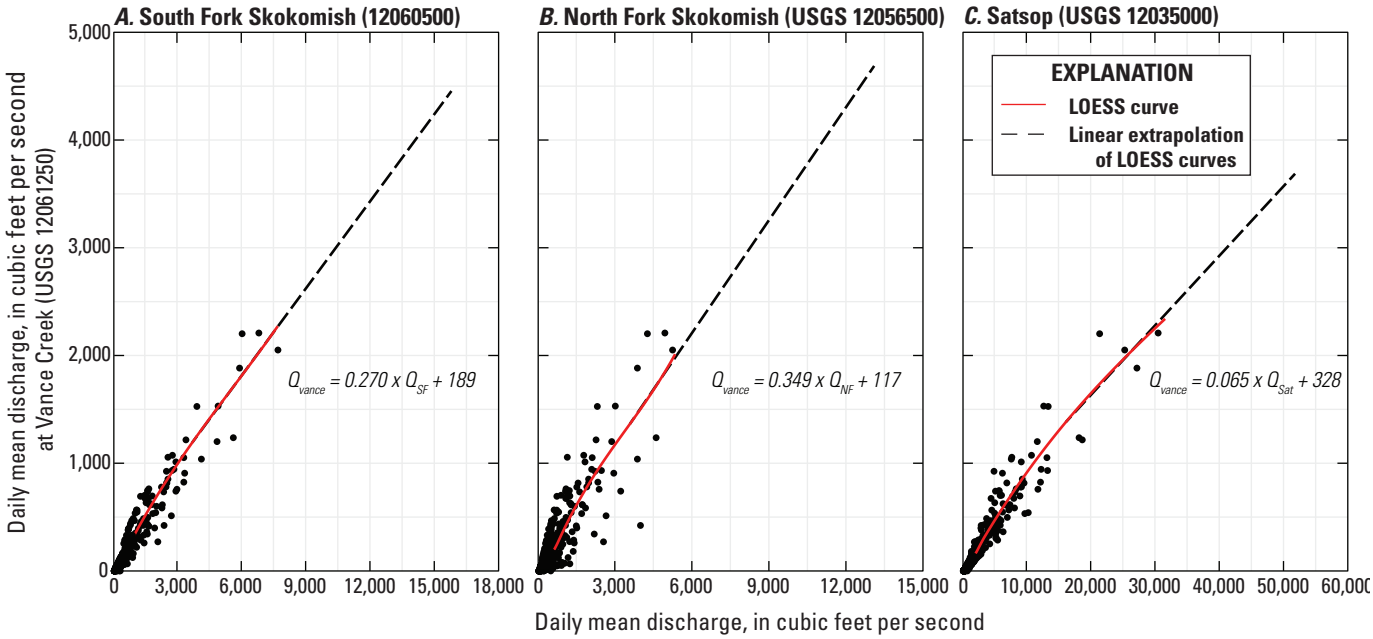

Figure 3. Graphs showing relations between daily mean discharge at Vance Creek and three reference streamgages, western Washington. *A*, South Fork Skokomish River near Union (USGS 12060500). *B*, North Fork Skokomish River below Staircase Rapids (USGS 12056500). *C*, Satsop River near Satsop (USGS 12035000). Equations for the linear extrapolation of the discharge relations are shown in each panel.

Sediment-Sampling Methods

Bedload Samples

Bedload samples were collected over 3 days in water year 2019 and 4 days in water year 2020. Bedload sampling was conducted using a Toutle River II pressure-difference bedload sampler, with a 12×6-inch (in.) (305×152-mm) opening and a mesh bag with 0.02-in. (0.5-mm) openings (Childers, 1999). Bedload sampling entailed lowering the sampler to the river bed and letting it rest there for a specified amount of time; each such lowering is referred to as a vertical. Multiple verticals across the sampling section were collected to form a composite bedload sample, called a transect. Throughout this report, the composite results from each transect are considered a single bedload sample (single equal width increment sampling method; Edwards and Glysson, 1999). Five to nine bedload samples were collected during each sampling day, with 50 unique samples collected in total. Samples were collected over a range of discharge from 511 to 2,940 ft^3/s (table 1). Most transects involved 9 or 10 equally spaced verticals spanning the width of the wetted channel; one sampling day (December 20, 2019) included transects with 5 verticals over only the middle of the channel, where essentially all bedload samples were collected. Sampler rest times on the bed ranged from 15 to 60 seconds, dependent on the intensity of bedload transport.

All material collected over each transect was composited, dried, and sieved to obtain final estimates of sample mass, split into full-ϕ size classes. Samples from December 11–13, 2019, were processed by the U.S. Geological Survey's–Cascades Volcano Observatory (USGS–CVO) sediment laboratory. All subsequent samples were processed by the USGS–Washington Water Science Center (USGS-WAWSC) sediment laboratory. Cross-laboratory comparison of samples from December 11, 2019, indicated that the two processing laboratories provided equivalent results (appendix 1).

The bedload flux for a given transect was estimated using the single equal width increment method (Edwards and Glysson, 1999) and calculated using the formula:

$$Q_{bl} = \frac{M}{T} \times \frac{W}{S_w n} \quad (1)$$

where

Q_{bl} is the bedload flux, in pounds per second,
M is the total sample mass, in pounds (lbs),
T is the bed rest time, in seconds,
W is the total cross section width, in feet,
S_w is the sampler width, in feet, and
N is the number of verticals collected over the transect.

Table 1. Summary data of bedload samples, Vance Creek, western Washington.

[Start and End Time: PDT, Pacific Daylight Time. **Abbreviations:** ft, foot; ft³/s, cubic foot per second; lb/s, pound per second; sec, second]

Start time (PDT)	End time (PDT)	Number of verticals	Bed rest (sec)	Sample width (ft)	Discharge (ft³/s)	Bedload flux (lb/s)
December 11, 2018						
11:20	11:50	5	60	80	511	0.0
13:05	13:30	5	60	80	666	7.7
13:35	13:50	5	60	80	752	10.7
13:55	14:33	9	60	80	841	14.6
14:41	15:21	9	60	80	952	31.5
15:35	16:00	9	30	80	1,080	52.7
09:55	10:25	10	20	99	1,835	39.7
10:40	11:15	10	20	99	1,875	103
11:30	11:54	10	20	99	1,980	25.0
12:04	12:46	10	20	99	2,017	96.4
13:36	14:10	10	20	99	2,120	57.4
14:17	14:48	10	20	99	2,065	27.4
15:00	15:32	10	20	99	2,070	13.3
15:55	16:39	10	20	99	1,980	109
December 18, 2018						
09:58	10:30	10	20	96	1,690	6.8
10:44	11:20	10	30	96	1,647	15.0
11:30	12:09	10	30	96	1,595	11.8
13:05	13:45	10	45	96	1,565	11.3
13:55	14:34	10	60	96	1,547	18.7
14:40	15:19	10	60	96	1,490	21.0
15:25	16:00	10	60	96	1,495	26.5
16:05	16:29	10	30	96	1,470	20.0
December 20, 2019						
10:40	11:00	10	20	92	785	2.4
11:06	11:40	10	60	92	777	7.3
12:20	12:40	5	60	45	785	0.2
12:42	12:56	5	60	45	795	3.9
13:00	13:17	5	60	45	785	4.4
13:20	13:45	5	60	45	779	9.3
13:50	14:09	5	60	45	779	7.3
14:31	14:48	5	60	45	769	4.0
14:50	15:15	5	60	45	764	9.1
January 7, 2020						
10:30	11:15	10	15	90	2,385	47.5
11:45	12:15	10	15	90	2,350	13.8
12:45	13:04	10	15	90	2,290	25.6
13:10	13:35	10	20	90	2,310	26.8
13:37	14:00	10	20	90	2,330	12.6
14:00	14:25	10	20	90	2,260	22.1
January 23, 2020						

Table 1. Summary data of bedload samples, Vance Creek, western Washington.—Continued

[Start and End Time: PDT, Pacific Daylight Time. **Abbreviations:** ft, foot; ft³/s, cubic foot per second; lb/s, pound per second; sec, second]

Start time (PDT)	End time (PDT)	Number of verticals	Bed rest (sec)	Sample width (ft)	Discharge (ft³/s)	Bedload flux (lb/s)
January 23, 2020—Continued						
11:20	12:03	10	15	90	2,500	86.0
12:05	12:31	10	15	90	2,585	36.5
12:47	13:30	10	15	90	2,715	97.6
13:35	14:02	10	20	90	2,845	21.8
14:05	14:36	10	20	90	2,940	26.7
14:38	15:08	10	20	90	2,900	50.4
February 7, 2020						
11:03	11:26	10	15	88	2,430	11.7
11:32	11:48	10	15	88	2,380	22.5
11:50	12:08	10	20	88	2,320	12.1
12:15	12:31	10	20	88	2,250	5.9
12:33	12:55	10	30	88	2,240	10.5
12:57	13:20	10	30	88	2,210	29.4
13:21	13:43	10	30	88	2,140	14.4

Suspended-Sediment Samples

Seven suspended-sediment concentration (SSC) samples were collected for this study, one on each of the 7 sampling days. SSC samples were collected using equal-width or equal-discharge increment sampling methods, using a D-74 isokinetic sediment sampler (Edwards and Glysson, 1999). All suspended-sediment samples involved collection of duplicate A and B samples to assess consistency of the results. Samples were analyzed at the USGS–CVO sediment laboratory to determine SSC and the fraction of suspended material less than (<) 0.063 mm in diameter. Duplicate A and B samples were averaged to get a final SSC and average fraction finer than 0.063 mm for each sampling event.

Bed Material Samples

Samples of the local channel bed material on exposed bars were collected for comparison with bedload samples. Bed material was sampled at two sites; one just downstream from the Skokomish Valley Road bridge, and one a few hundred yards upstream from the bridge (fig. 1*A*). Surface bed-sediment grain-size distributions were characterized using Wolman pebble counts (Wolman, 1954); two 100-clast counts (samples 1a and 1b) were collected at the downstream site and one 100-clast count (sample 2) was collected at the upstream site. Clasts were randomly selected using a 100-ft tape extended along river-parallel transects over the axis of low gravel bars.

Subsurface bed-sediment grain-size distributions were determined using bulk sieving methods after first removing the surface layer to a depth roughly equivalent to the diameter of the largest clasts on the surface. Subsurface samples were collected at the midpoint of the pebble counts. Two subsurface samples were collected at the downstream site, each weighing about 125 lb. A single 140-lb sample was collected at the upstream site. Subsurface material coarser than 0.63 in. (16 mm) was sieved and weighed in the field. All material finer than 0.63 in. was retained and returned to the laboratory, where it was dried, split down to a 6- to 8-lb subsample, and sieved at full-ϕ intervals down to 0.02 in. (0.5 mm).

The difference between the wet field weight and dry laboratory weight of the < 0.63 in. material was used to correct for the water weight contained in the samples; we assumed that water was predominantly held in the < 0.63 in. size classes and did not markedly affect the weights of the greater than (>) 0.63 in. material weighed in the field. Water accounted for 1 to 3 percent of the total sample weights.

Sediment Rating Curves and Uncertainty

Bedload Rating Curve

Bedload flux is often characterized as a power function of the shear stress in excess of what is needed to initially mobilize particles (Meyer-Peter and Müller, 1948; Wiberg and Dungan Smith, 1989). Following in that vein, the relation between discharge and measured bedload flux in Vance Creek was fit using a threshold power law of the form

$$Q_{bl} = a(Q - Q_c)^b \quad (2)$$

where

Q_{bl} is the bedload flux, in pounds per second,
Q is the discharge, in ft^3/s,
Q_c is a threshold discharge below which no transport is assumed to occur (that is, if $Q < Q_c$, $Q_{bl} = 0$),

and a and b are constants estimated through regression.

A threshold discharge of 400 ft^3/s was selected, based on observations of minimal transport at 500 ft^3/s; this is equivalent to a critical Shields stress of 0.035 (depth = 1.5 ft, slope = 0.0042, D_{50} = 0.115 ft). This Shields stress value is similar to the critical Shields stress of 0.039 that would be predicted just based on local slope (Lamb and others, 2008).

Ordinary least squares regression (OLS) on log-transformed variables was used to estimate the a and b parameters in equation 2. Duan's (1983) smearing estimate was used to account for bias in back-transformed estimates of flux rates. The final rating curve estimated using this process was

$$Q_{bl} = 0.0180\,(Q - 400)^{0.978} \times 1.394 \quad (3)$$

where

Q is the unit-value (15-minute) discharge, in cubic feet per second, and the trailing value of 1.394 is the bias correction factor.

In cases where $Q < 400$, Q_{bl} is assumed to be 0.

Rating curve relations between sediment flux and discharge are often non-linear. Consequently, sediment loads estimated from all 15-minute discharge records on a given day are often different than loads estimated based on the daily mean discharge for that day. This is particularly true in flashy systems like Vance Creek, where peak-flow events typically rise and fall in a single day. However, in Vance Creek, the estimated relation between discharge and bedload transport is nearly linear ($Q_{bl} \sim Q^{0.978}$); consequently, application of equation 3 to 15-minute discharge records or daily mean discharge records produces essentially identical results. Equation 3 is then considered valid for use with 15-minute or daily mean discharge values.

There is substantial scatter in the relation between bedload flux and discharge over individual sampling days. This scatter is due to some combination of sampling error and true short-term variability in the bedload flux (for examples, Iseya and Ikeda, 1987; Recking and others, 2009). Averaging the data over individual sampling days reduces, but does not eliminate, this variability. Average bedload fluxes were notably higher for the first two sampling days (December 11 and 13, 2018) than subsequent sampling days at similar discharges (fig. 4, inset graph). This apparent shift in the bedload-discharge relation coincides with substantial scouring of the channel during the December 13, 2018, high-flow event, documented through changes in the stage-discharge relation at the Vance Creek streamgage. These observations underscore that the relation between discharge and bedload is complex and variable over both short (hours, days) and long (months to decades) time periods. The rating curve presented here likely provides a reasonable estimate of the average discharge-bedload relation over the study period but likely is less accurate when applied to time periods outside of that study period.

Suspended-Sediment Concentration Rating Curves

The seven collected SSC samples do not show a consistent relation to discharge (fig. 5*A*), and the fit to these data based on simple OLS regression resulted in a fitted exponent of < 1, which was determined to be implausible. For a given discharge, the two samples collected during periods of increasing discharge (December 11, 2018, and January 23, 2020) were noted to have substantially higher SSC values than samples collected when discharge was either stable or decreasing (table 2). This pattern of higher or lower SSC values suggests a clockwise hysteresis in the concentration-discharge relation (Bača, 2008). SSC was then estimated using an equation of the form

$$SSC = 10^{[a+c(inc)]} Q^b \quad (4)$$

where

SSC is the suspended-sediment concentration, in milligrams per liter,
Q is the discharge, in ft^3/s, and
inc is a dummy variable that takes a value of 1 if discharge is increasing substantially, and a value of 0 when discharge is stable or decreasing.

OLS on log-transformed variables was used to estimate the a, b, and c parameters in this equation. Duan's (1983) smearing estimate was used to account for bias in back-transformed estimates of SSC. The final rating curve estimated using this process was

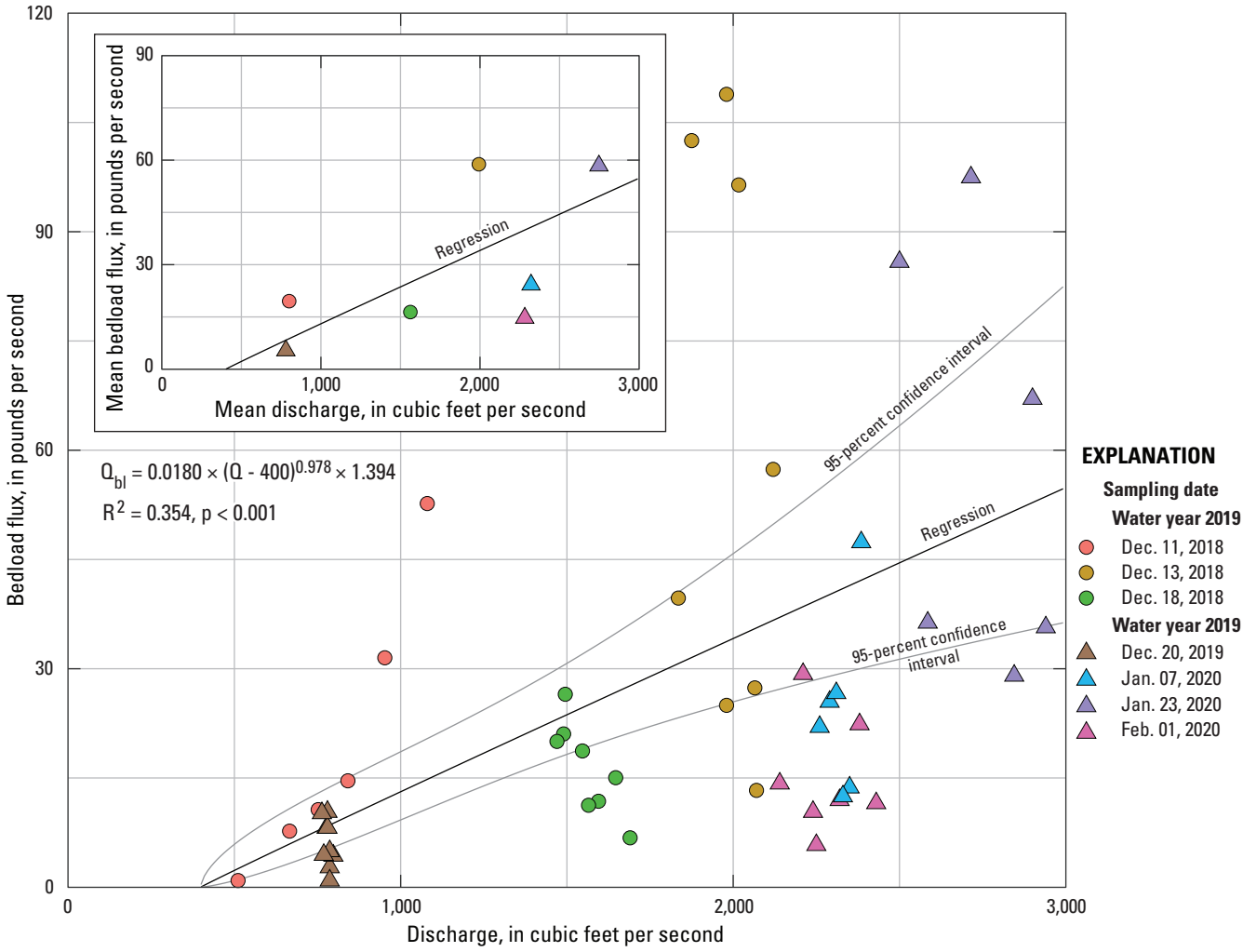

Figure 4. Graph showing relation between bedload flux and discharge at Vance Creek (USGS streamgage 12061250), western Washington. Fitted thresholded power law and 95-percent confidence intervals shown. Inset graph shows samples averaged by sampling date with same power law fit as in the main panel.

$$SSC = \begin{cases} 0.00975\,Q^{1.271} \times 1.065 \\ \text{if discharge is steady or decreasing} \\ 0.0397\,Q^{1.271} \times 1.065 \\ \text{if discharge is increasing} \end{cases} \quad (5)$$

where the trailing value of 1.065 is the bias correction factor.

Equation 5 predicts that, for a given discharge, SSC would tend to be about four times higher when discharge is increasing relative to periods when discharge was steady or decreasing.

Once SSC values for each 15-minute discharge value have been estimated, suspended-sediment loads (SSL) can be calculated using the formula

$$SSL = SSC \times Q \times k \quad (6)$$

where

SSL is the suspended-sediment load, in tons per 15-minute discharge interval, and

k is a conversion factor (2.809×10^{-5}) accounting for unit transformations (Rasmussen and others, 2009).

To develop a relation between discharge and SSC that could be applied to daily mean discharge records, we first used equations 5 and 6 to estimate suspended-sediment loads at 15-minute intervals. For these estimates, the dummy variable *inc* was set to 1 for 15-minute discharge values where discharge was greater than 200 ft^3/s and had increased more than 5 percent over the preceding hour.

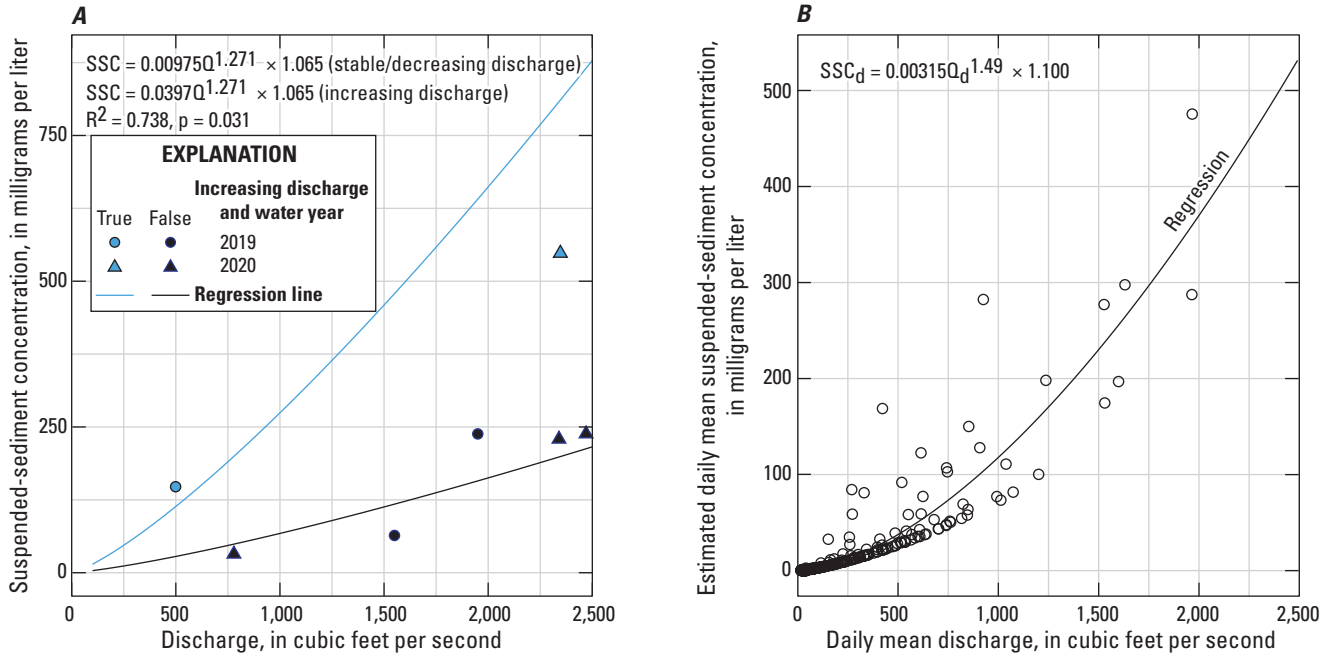

Figure 5. Graphs showing suspended-sediment concentration (SSC) rating curves, Vance Creek, western Washington. *A*, relation between sampled SSC and discharge. Points have been split depending on whether they were sampled during periods of rapidly increasing discharge or during periods of steady or decreasing discharge. *B*, relation between estimated daily mean SSC and daily mean discharge; daily SSC values are based on regressions shown in graph *A* applied to the available 15-minute discharge records.

Estimated suspended-sediment loads at 15-minute intervals were summed to get daily loads, and equation 6 was used to back-calculate a daily mean SSC, referred to as SSC_d.

A relation between SSC_d and daily mean discharge (Q_d) of the form

$$SSC_d = a Q_d^b \quad (7)$$

was then estimated using the same OLS methods previously described (fig. 5*B*). This resulted in a final equation of

$$SSC_d = 0.00315 Q_d^{1.49} \times 1.100 \quad (8)$$

where the trailing 1.100 is the bias correction factor.

Daily SSL, in tons per day, can then again be calculated using equation 6, but with a k value of 0.002697 to convert values to tons per day, instead of the previous k value used to convert to tons per 15-minute interval.

Uncertainty in Estimated Sediment Loads

Uncertainties in rating-curve estimates of sediment load were quantified using statistical methods described in Gilroy and others (1990). These estimates assume that the variance of the available samples provide a reasonable estimate of the true population variance. This assumption is plausible when the bedload-rating curve is used to estimate bedload flux over the 2-year study period. However, given the possibility of systematic changes in the relation between discharge and bedload flux over periods of years or decades, these uncertainty bounds likely underestimate uncertainty when the regressions are applied to the long-term daily discharge record.

The small number of suspended-sediment samples leaves the substantial uncertainty in estimated suspended-sediment fluxes, particularly given the scatter observed in the available samples. Moreover, the available samples are likely insufficient to accurately characterize variance. As a result, uncertainties calculated using the previously described methods are likely optimistic. Because the data used to fit equation 8 were themselves derived from a previous regression, as opposed to actual samples, the statistical methods for uncertainty provide meaningless results. For all the previously stated reasons, uncertainty in long-term estimates of suspended-sediment loads is likely large—on the order of ± 50 percent—but not explicitly calculated.

Table 2. Summary data of suspended-sediment samples, Vance Creek, western Washington.

[Start and End Time: PDT, Pacific Daylight Time. Sample method: EDI, equal-discharge increment method; EWI, equal-width increment method. **Abbreviations and symbols:** ft^3/s, cubic foot per second; lb/s, pound per second; mg/L, milligram per liter; mm, millimeter; <, less than]

Date	Start time (PDT)	End time (PDT)	Sample method	Discharge (ft^3/s)	Suspended-sediment concentration duplicate samples (mg/L)			Fraction < 0.063 mm duplicate samples			Rising limb?
					A set	B set	Average	A set	B set	Average	
Dec. 11, 2018	11:02	11:57	EWI	499	127	168	148	51	50	50	Yes
Dec. 13, 2018	11:03	11:19	EDI	1,950	236	241	238	46	46	46	No
Dec. 18, 2018	12:42	13:08	EDI	1,550	66.2	61.8	63.9	61	61	61	No
Dec. 20, 2019	14:03	14:21	EDI	779	27.2	39.4	33.3	59	41	47	No
Jan. 07, 2020	12:17	12:36	EDI	2,340	233	228	231	55	53	54	No
Jan. 23, 2020	10:25	11:01	EDI	2,350	544	555	549	48	48	48	Yes
Feb. 01, 2020	10:37	11:02	EDI	2,470	240	240	240	51	49	50	No

Vance Creek Sediment Loads

Bedload

Annual bedload fluxes for water years 2019 and 2020 were estimated to be 11,000 ± 2,000 and 14,400 ± 2,100 tons, respectively, based on application of equation 3 to the available 15-minute discharge records (fig. 6). Application of equation 3 to the extended daily discharge record results in an estimated mean annual bedload flux of 12,200 ± 2,300 tons over water years 1930–2020. Over that extended period of record, estimated annual bedload fluxes ranged from as little as 630 ± 240 tons, in water year 2001, to as much as 27,300 ± 4,400 tons in water year 1999. Typical estimated annual flux (16th to 84th percentile range) ranged from 6,100 to 19,900 tons.

Bedload Grain-Size Distribution

Sampled bedload material was predominantly pebbles and cobbles from 0.08 to 2.5 in. (2 to 64 mm) in diameter (fig. 7*A*). Median particle diameters (D_{50}) were typically from 0.2 to 1.4 in. (5 to 35 mm), while 84th percentile particle diameters (D_{84}) were generally from 0.4 to 3.1 in. (10 to 80 mm; figs. 7*B* and 7*C*). There is a trend of increasing D_{50} and D_{84} values with increasing discharge although with substantial scatter, particularly for the D_{50}. For a given discharge, there is no discernible relation between bedload flux and grain size—the substantial short-term variability in flux rates observed in figure 4 thus cannot be explained in terms of variations in sediment size of the load. Sand typically comprised 5–20 percent of the bedload material.

Comparisons with the Channel Bed Material

The channel bed material near the sampling site was predominantly gravel from 0.08 to 5.00 in. (2 to 128 mm) in diameter, with the largest clasts falling in the 7.1–10.1 in. (180–256 mm) size bin (fig. 8). Sand comprised 6 to 17 percent of the samples. Surface and subsurface grain-size distributions were very similar for samples 1a and 1b, collected downstream from the Skokomish Valley Road bridge, indicating little surface armoring. For sample 2, the subsurface was modestly depleted in the 0.32–1.26 in. (8–32 mm) size range and relatively enriched in the 0.08–0.32 in. (2–8 mm) size range in comparison to the surface, although the distributions were similar over the coarse end. All samples were similar enough to each other that the three surface samples were averaged to create a single surface distribution, and the three subsurface samples likewise averaged to get one representative subsurface distribution (fig. 7).

The sampled bedload was typically finer than the surrounding channel bed material (fig. 8), consistent with laboratory and field observations that the time-integrated bedload flux of gravel bedded rivers is often modestly finer than the local channel subsurface material (Parker and Toro-Escobar, 2002). Regardless, nearly the full distribution of grain sizes present on the bed are mobilized, and in rough proportion to their abundance on the bed, at discharges of 2,500 ft^3/s.

Suspended-Sediment Loads

Application of equation 5 to the available 15-minute discharge records results in estimated annual suspended-sediment flux of 6,600 ± 2,500 tons in water year 2019 and 11,000 ± 3,800 tons in water year 2020. To those estimations, periods of increasing discharge were defined as those where the discharge was greater than 200 ft^3/s and had increased at least 5 percent over the preceding hour. Application of equation 6 to the 1930–2020 period of estimated daily mean discharge resulted in an estimated mean annual suspended-sediment flux of about 9,000 tons/year; uncertainty is estimated to be on the order of ± 50 percent. SSC samples consistently contained 50 percent sand and 50 percent silt and clay, regardless of sampling discharge (table 2).

Ratios of Bedload to Total Sediment Load

Bedload and suspended load are two distinct modes of sediment transport that, in combination, make up a river's total sediment load (Einstein, 1950; Turowski and others, 2010; dissolved load is not considered here). The relative partitioning of the total sediment load between the two transport modes is a common measure of river condition (Turowski and others, 2010). In order to estimate 'observed' load partitioning based directly on sample data, we paired each SSC measurement with an estimate of the concurrent bedload flux based on the average flux from the two bedload samples made most closely in time to the SSC sample, as well as the average bedload flux over the full sampling day. The two approaches for pairing SSC data with a concurrent bedload flux gave materially similar results, and load partitions based on the daily average bedload flux are shown here.

The fraction of the total sediment load carried as bedload generally decreased with increasing discharge, particularly above 2,000 ft^3/s (fig. 9). Bedload constituted about 75 percent of the total flux at relatively low (< 1,000 ft^3/s) flows, decreasing to about 65 percent at 2,000 ft^3/s and down to about 30 percent at around 2,500 ft^3/s. Bedload to total load ratios also were calculated based on time-integrated fluxes estimated in the preceding sections; bedload averaged 58 percent of the total flux estimated using both the available 15-minute discharge records and extrapolated daily discharge records.

A global compilation of load portioning by Turowski and others (2010) found that, for sites with similar drainage area as Vance Creek, bedload constituted an average of about 30 percent of the total load, with an upper limit of about 68 percent. With bedload making up about 60 percent of its total load, Vance Creek thus carries a high, but not globally unprecedented, fraction of its total sediment load as bedload.

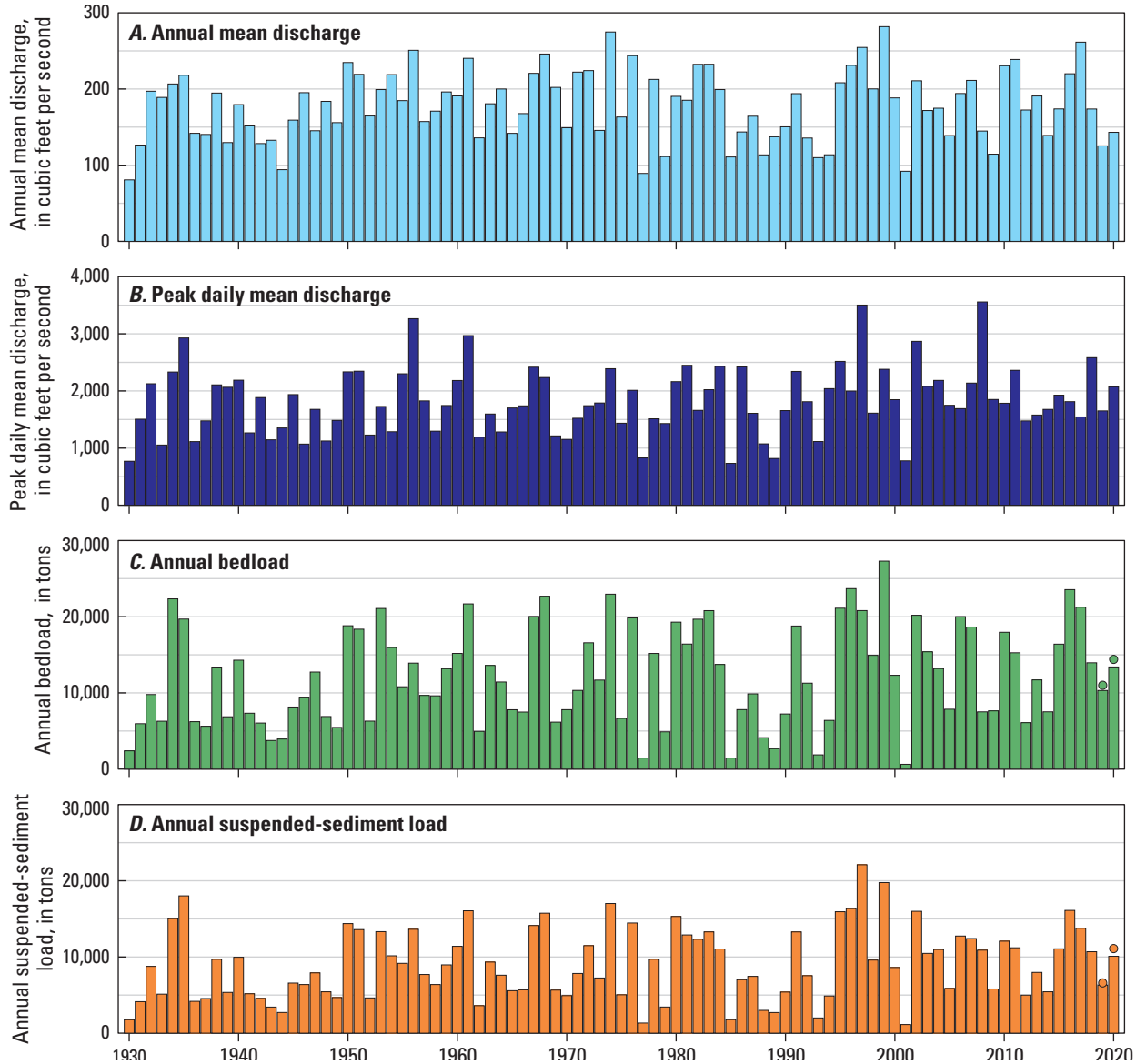

Figure 6. Graphs showing estimated long-term discharge and suspended-sediment load characteristics for Vance Creek, western Washington, 1930–2020. Loads in graphs *C* and *D* are based on application of sediment-rating curves to extrapolated daily mean discharge record. Annual loads estimated for water years 2019–20 based on available 15-minute discharge records are shown as filled circles in graphs *C* and *D* for comparison.

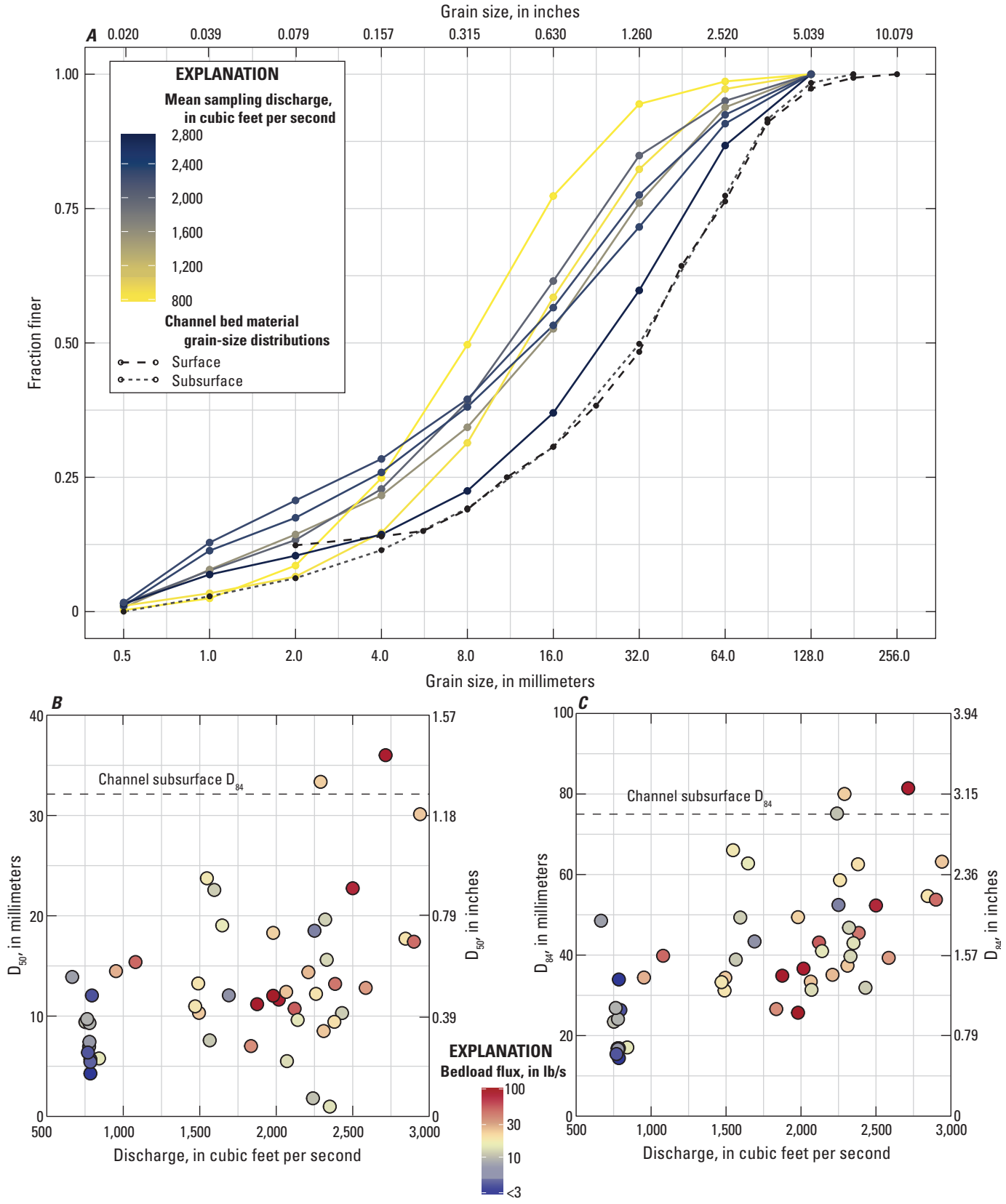

Figure 7. Graphs showing grain-size distribution of bedload samples, Vance Creek, western Washington. *A*, grain-size distribution of sampled bedload, aggregated by day. *B*, median (D_{50}) particle diameter for each bedload sample plotted against discharge. Point fill color indicates bedload flux. *C*, as per graph *B*, but for the 84th percentile grain-size diameter (D_{84}).

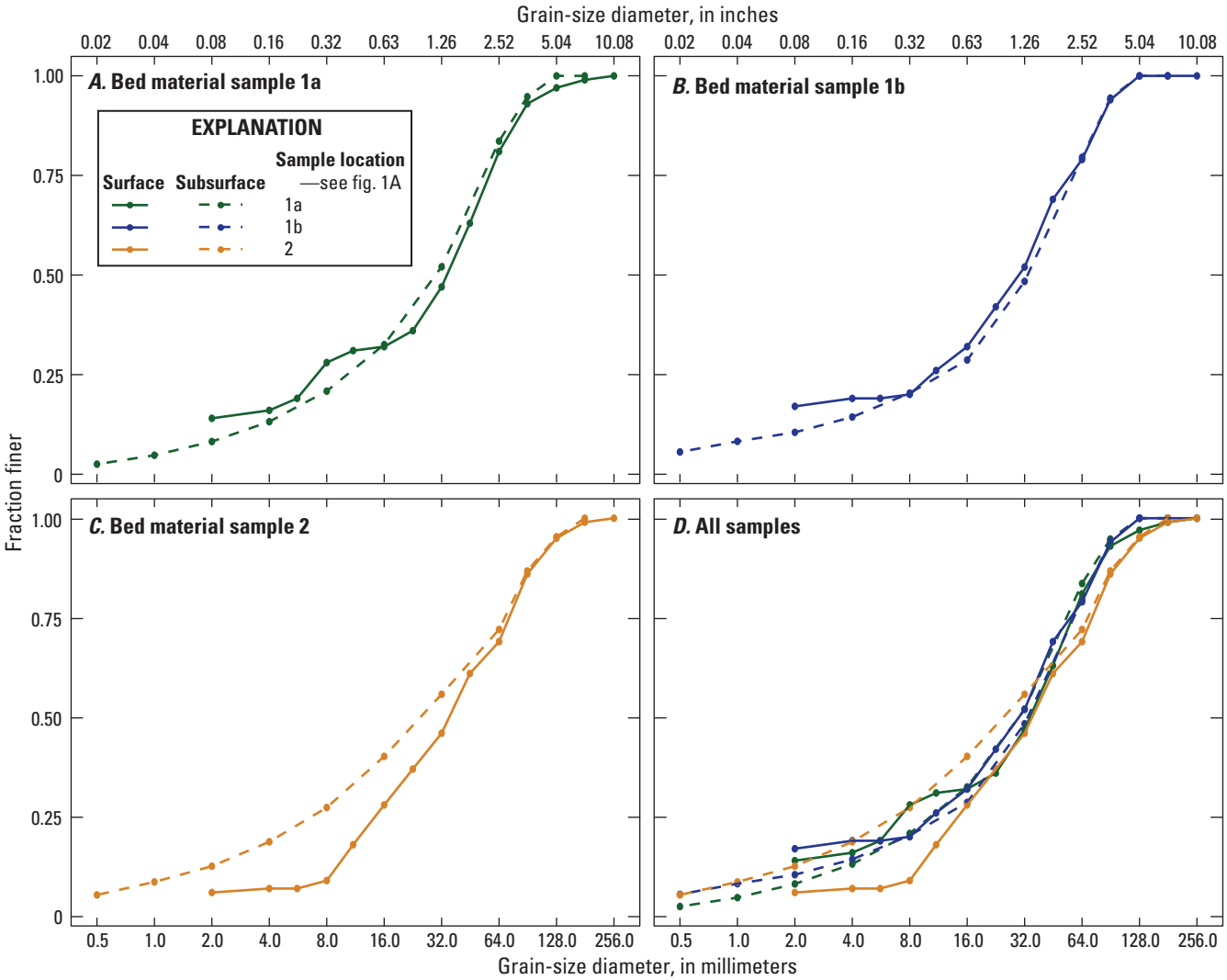

Figure 8. Graphs showing grain-size distributions for surface and subsurface channel bed material of Vance Creek near the sampling site, western Washington. Locations of samples are shown in figure 1*A*.

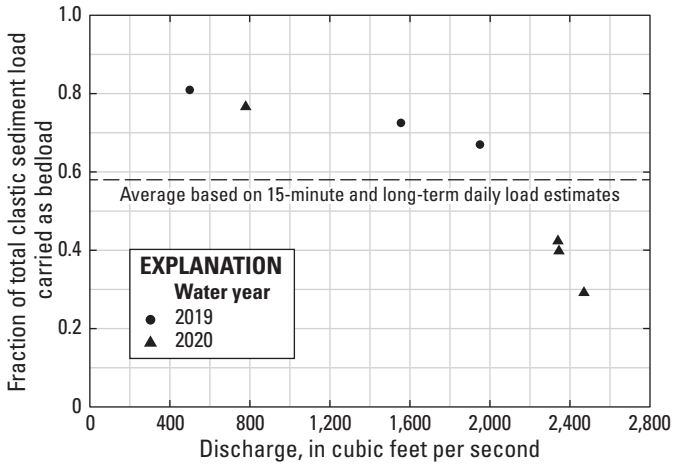

Figure 9. Graph showing fraction of total sediment load carried as bedload, based on discrete samples (points) and the integrated average based on 15-minute and daily sediment load estimates (dashed line), Vance Creek, western Washington.

Comparison of Sediment Loads in Vance Creek with Nearby Basins

The sediment loads measured at Vance Creek were compared to five nearby river basins where various amounts of bedload and suspended-sediment load data were available (see fig. 1*C*)—(a) main stem Skokomish River (streamgage 12060500); (b) South Fork Skokomish River, upstream from the Vance Creek confluence; (c) North Fork Skokomish River (streamgage 12056500) upstream of the Cushman Dam complex; (d) Elwha River (streamgage 12044900) upstream of the (now removed) Glines Canyon Dam, and (e) Dungeness River (streamgage 12048600), a few miles upstream from its mouth in the Straits of Juan de Fuca (fig. 1*C*; table 3). Data are most complete for the main stem Skokomish, upper Elwha, and Dungeness River sites.

Information about sediment transport in the lower Skokomish River is based on sediment loads presented in Collins and others (2019) whereas grain-size information is based on the raw measurement data available in the USGS National Water Information System (NWIS) (U.S. Geological Survey, 2020). Sediment loads for the upper Elwha River are based on data presented in Curran and others (2009), with grain-size information again based on raw measurement data stored in NWIS. All sediment-load data for the Dungeness and North Fork Skokomish Rivers were based purely on an analysis of the available measurements in NWIS. Simons and Associates, Inc. (1994) collected eleven paired bedload and suspended-sediment samples at a site in the South Fork Skokomish River and six at a site in the North Fork Skokomish River; the average bedload to total sediment load ratio, weighted by total measured flux, of these samples was used as an approximation of the long-term load partitioning. New analyses of available data conducted as part of this study are presented in appendix 2.

Several approaches were used to compare average annual sediment loads across these drainage basins, which have different drainage areas and runoff depths (table 3). First, mean sediment loads were divided by upstream contributing area to get mean sediment yields, in tons per square mile per year [tons/mi^2/year]; these yield values account for the different sizes of the basins. Second, mean annual sediment loads were divided by mean annual runoff volume to get a mean sediment concentration, expressed in milligrams per liter [mg/L]. Because runoff volume is a function of both drainage area and average precipitation, normalizing by runoff volume simultaneously accounts for cross-basin variations in both (Mueller and Pitlick, 2013).

Bedload yields for the Vance Creek site (589 tons/mi^2/year; table 4) were similar to yields at the Skokomish (591 tons/mi^2/year) and upper Elwha River sites (540 tons/mi^2/year). The Dungeness River was markedly lower at 107 tons/mi^2/year. The fivefold lower bedload yield at the Dungeness River site is proportional to the relatively lower runoff depth in that drainage basin, which sits in the rain shadow of the Olympic Mountains (table 3). Mean bedload concentrations across the four sites fall in a relatively narrow range between 44 and 109 mg/L; the Vance Creek site has an intermediate value in this range, at 69 mg/L.

In contrast, suspended-sediment yields at the Vance Creek site, at 435 tons/mi^2/year, are similar to yields at the Dungeness River site despite the markedly lower runoff from the latter basin, and about five times lower than yields at the Skokomish and upper Elwha River sites (table 4). Cast in terms of mean suspended-sediment concentrations, Vance Creek has substantially lower concentrations than the Skokomish, Elwha, or Dungeness Rivers; however, mean SSC in the North Fork Skokomish River is lower still.

At the Skokomish, upper Elwha, Dungeness, and South Fork Skokomish River sites, bedload constituted between 21 to 29 percent of the total long term sediment load (table 4). These values are similar to global averages for drainage basins with similar drainage areas (Turowski and others, 2010). The available data suggest that bedload makes up a relatively small fraction of the total sediment load passing the North Fork Skokomish River site (3 percent), though this is based on a small set of paired samples. In contrast, bedload contributes nearly 60 percent of the total load at the Vance Creek site. This high percentage places Vance Creek near the upper limit of data observed globally (table 4; Turowski and others, 2010). The bedload at Vance Creek is also notably less sand-rich than at other sites; sand constitutes 13 percent of the bedload flux at Vance Creek, compared with 20 to 37 percent of the load at the comparison sites.

Table 3. Physical and hydrologic characteristics of comparison basins.

[0.5 AEP based on reported or estimated values from Mastin and others, 2016 **Abbreviations:** AEP, annual exceedance probability; ft^3/s, cubic foot per second; in., inch; in./d, inch per day; mg/L, milligrams per liter; mi^2, square mile; no., number; USGS, U.S. Geological Survey]

Sampling site (fig. 1C)	USGS streamgage no.	Drainage area (mi^2)	Period of record (water years)	Mean annual flow (ft^3/s)	mean annual runoff depth (in.)	0.5 AEP peak-flow (ft^3/s)	0.5 AEP peak-flow runoff depth (in./d)	Local channel slope (percent)
Vance Creek	***12061250***	***20.7***	***[1]1930–2020***	***178***	***117.0***	***2,240***	***4.02***	***0.42***
Skokomish River, Hwy101	12060500	227	1944–2020	1250	74.8	12,000	1.97	0.05
Elwha River	12044900	198	1995–97, 2005–11	1367	93.8	13,000	2.44	0.26
Dungeness River	12048600	178	1924–28, 1938–2020	441	33.7	3,120	0.65	1.16
North Fork Skokomish River	12056500	56.7	1925–2020	517	123.9	6,950	4.56	0.67
South Fork Skokomish River (bridge near Browns Camp)	[2]12060500	51.6	1932–84, 1996–2020	491	129.3	6,710	4.56	0.53

[1]Daily discharge record extrapolated from regression with nearby gages.

[2]Sediment sampling site is upstream of noted streamgage. Mean annual flow is estimated based on drainage area ratio of the sampling site and the 12060500 streamgage (0.68). The 0.5 AEP value is based on a peak-flow scaling approach described in Mastin and others (2016).

Table 4. Sediment flux characteristics of comparison basins.

[Global average for drainage area is based on Turworski and others (2010, equation 7). **Abbreviations:** --, No Data; D_{50}, median particle diameter; D_{84}, 84th percentile particle diameter; mg/L, milligrams per liter; mm, millimeters; no., number; ton/mi²/y, ton per square mile per year; USGS, U.S. Geological Survey]

Sampling site (fig. 1C)	USGS streamgage no.	Mean sediment yield (ton/mi²/y)		Mean sediment concentration (mg/L)		Percentage of total load carried as bedload		Bedload grain size			Source
		Bedload	Suspended load	Bedload	Suspended load	Measured	Global average for drainage area	Sand fraction (percent)	D_{50} (mm)	D_{84} (mm)	
Vance Creek	***12061250***	***589***	***435***	***69***	***51***	***58***	***29***	***13***	***15.5***	***44***	***This report***
Skokomish River, Hwy 101	12060500	591	2033	109	374	23	19	20	6.2	18	Collins and others, 2019; U.S. Geological Survey, 2020
Upper Elwha River	12044900	540	1993	79	293	21	20	35	4.2	19	Curran and others, 2009
Dungeness River	12048600	107	338	44	139	24	20	37	5.5	40	U.S. Geological Survey, 2020
North Fork Skokomish River	12056500	--	111	--	12	[1]3	25	--	--	--	Simons and Associates, Inc., 1994
South Fork Skokomish River (bridge near Browns Camp)	--	--	--	--	--	[1]29	25	--	--	--	Simons and Associates, Inc., 1994

[1]Values are flux-weighted mean partitioning, based on available paired bedload and suspended sediment measurements.

Taken together, these comparisons suggest that bedload fluxes at this Vance Creek site are relatively consistent with other basins in the region, after considering differences in drainage area and average runoff. In contrast, fine sediment loads in Vance Creek are relatively low. This is apparent both in terms of the suspended-sediment loads and the low fraction of sand in Vance Creek bedload samples. Observations in the North Fork Skokomish River indicate that the low suspended-sediment yields in Vance Creek are not, in and of themselves, out of the norm for the region. However, Vance Creek carries an unusually large fraction of its total sediment load as bedload, deviating from trends observed both within the region and in global compilations.

Summary

Bedload and suspended-sediment samples collected at a site in lower Vance Creek during water years 2019–20 were used to characterize local sediment-transport conditions. Over the period of extrapolated daily discharge records (water years 1930–2020), the mean annual bedload flux was estimated to be 12,200 ± 2,300 tons per year; that load is composed primarily of gravel from 0.08 to 2.5 in. (2 to 64 millimeters) in diameter and about 13 percent sand. The grain-size distribution of the bedload was similar to, but somewhat finer than, the local channel bed material, coarsening with increasing discharge. Suspended-sediment loads over the 1930–2020 time period were estimated to average 9,000 tons per year; limited data precluded a precise estimate of uncertainty bounds around this value, but uncertainty could be as large as ± 50 percent. The suspended load was of composed of 50 percent silt and clay and 50 percent sand at all sampled discharges. Over the long term, bedload is estimated to make up about 60 percent of the river's total sediment load; this value is near the upper limit observed in a global compilation of load partitions.

A comparison of sediment loads from several nearby sites indicates that bedload flux at this Vance Creek site is reasonably typical of the region but that the fine-sediment loads, both in terms of suspended-sediment loads and the sand fraction of the bedload material, are relatively low. Although the suspended-sediment yields and mean concentrations of Vance Creek are not, in and of themselves, outside the range observed regionally, they are notably low given the relatively abundant bedload transport.

References Cited

Bača, P., 2008, Hysteresis effect in suspended sediment concentration in the Rybárik basin, Slovakia: Hydrological Sciences Journal, v. 53, no. 1, p. 224–235, accessed July 17, 2020, at https://doi.org/10.1623/hysj.53.1.224.

Bountry, J., and Godaire, J., 2011, Vance Creek Geomorphology and Modeling Report: Denver, Bureau of Reclamation Technical Report No. SRH-2011-08, 86 p.

Childers, D., 1999, Field comparisons of six pressure-difference bedload samplers in high-energy flow: U.S. Geological Survey Water Resources Investigations Report 92-4068, 71 p., accessed November 10, 2021, at https://doi.org/10.3133/wri924068.

Cleveland, W.S., and Devlin, S.J., 1988, Locally weighted regression—An approach to regression analysis by local fitting: Journal of the American Statistical Association, v. 83, no. 403, p. 596–610.

Collins, B.D., Dickerson-Lange, S.E., Schanz, S., and Harrington, S., 2019, Differentiating the effects of logging, river engineering, and hydropower dams on flooding in the Skokomish River, Washington, USA: Geomorphology, v. 332, p. 138–156, accessed September 16, 2020, at https://doi.org/10.1016/j.geomorph.2019.01.021.

Curran, C.A., Konrad, C.P., Higgins, J.L., and Bryant, M.K., 2009, Estimates of sediment load prior to dam removal in the Elwha River, Clallam County, Washington: U.S. Geological Survey Scientific Investigations Report 2009–5221, 18 p., accessed July 18, 2020, at https://doi.org/10.3133/sir20095221.

Duan, N., 1983, Smearing estimate—A nonparametric retransformation method: Journal of the American Statistical Association, v. 78, no. 383, p. 605–610.

Edwards, T.K., and Glysson, G.D., 1999, Field methods for measurement of fluvial sediment: U.S. Geological Survey Techniques of Water-Resources Investigations, book 3, chap. C2, 97 p, accessed September 12, 2020, at https://pubs.usgs.gov/twri/twri3-c2/html/pdf.html.

Einstein, H.A., 1950, The bed-load function for sediment transportation in open channel flows: United States Department of Agriculture, Washington, D.C., Technical Bulletin No. 1026, p. 25, accessed February 22, 2022, at https://naldc.nal.usda.gov/download/CAT86201017/PDF

Gilroy, E.J., Hirsch, R.M., and Cohn, T.A., 1990, Mean square error of regression-based constituent transport estimates: Water Resources Research, v. 26, no. 9, p. 2069–2077, accessed July 19, 2020, at https://doi.org/10.1029/WR026i009p02069.

Iseya, F., and Ikeda, H., 1987, Pulsations in bedload transport rates induced by a longitudinal sediment sorting—A flume study using sand and gravel mixtures: Geografiska Annaler. Series A. Physical Geography, v. 69, no. 1, p. 15–27, accessed September 10, 2020, at https://doi.org/10.1080/04353676.1987.11880193.

Lamb, M.P., Dietrich, W.E., and Venditti, J.G., 2008, Is the critical Shields stress for incipient sediment motion dependent on channel-bed slope?: Journal of Geophysical Research—Earth Surface, v. 113, no. F2, 20 p, accessed September 10, 2020, at https://doi.org/10.1029/2007JF000831.

Mastin, M.C., Konrad, C.P., Veilleux, A.G., and Tecca, A.E., 2016, Magnitude, frequency, and trends of floods at gaged and ungaged sites in Washington, based on data through water year 2014 (ver 1.2, November 2017): U.S. Geological Survey Scientific Investigations Report 2016–5118, 70 p., accessed February 22, 2022, at http://dx.doi.org/10.3133/sir20165118.

Meyer-Peter, E., and Müller, R., 1948, Formulas for bed-load transport, *in* International Association for Hydraulic Structures Research (IAHSR) 2nd meeting, June 7–9, 1984, Proceedings: Stockholm, IAHR, appendix 2, p. 39–64, accessed September 7, 2020, at https://repository.tudelft.nl/islandora/object/uuid:4fda9b61-be28-4703-ab06-43cdc2a21bd7.

Mueller, E.R., and Pitlick, J., 2013, Sediment supply and channel morphology in mountain river systems—1. Relative importance of lithology, topography, and climate: Journal of Geophysical Research—Earth Surface, v. 118, no. 4, p. 2325–2342, accessed September 10, 2020, at https://doi.org/10.1002/2013JF002843.

Parker, G., and Toro-Escobar, C.M., 2002, Equal mobility of gravel in streams—The remains of the day: Water Resources Research, v. 38, no. 11, p. 46-1–46-8, accessed July 18, 2020, at https://doi.org/10.1029/2001WR000669.

Rasmussen, P.P., Gray, J.R., Glysson, G.D., and Ziegler, A.C., 2009, Guidelines and procedures for computing time-series suspended-sediment concentrations and loads from in-stream turbidity-sensor and streamflow data: U.S. Geological Survey Techniques and Methods, book 3, chap. C4, 52 p, accessed July 18, 2020, at https://pubs.usgs.gov/tm/tm3c4/pdf/TM3C4.pdf.

Recking, A., Frey, P., Paquier, A., and Belleudy, P., 2009, An experimental investigation of mechanisms involved in bed load sheet production and migration: Journal of Geophysical Research—Earth Surface, v. 114, no. F3, 13 p, accessed September 18, 2020, at https://doi.org/10.1029/2008JF000990.

Simons and Associates, Inc., 1994, Draft Skokomish River sediment transport data report 1993–1994: Tacoma, Washington, City of Tacoma, Department of Public Utilities, 277 p.

Turowski, J.M., Rickenmann, D., and Dadson, S.J., 2010, The partitioning of the total sediment load of a river into suspended load and bedload—A review of empirical data: Sedimentology, v. 57, no. 4, p. 1126–1146, accessed October 19, 2020, at https://doi.org/10.1111/j.1365-3091.2009.01140.x.

U.S. Geological Survey, 2020, USGS water data for the Nation: U.S. Geological Survey National Water Information System database, accessed October 1, 2020, at https://doi.org/10.5066/F7P55KJN.

Washington State Department of Natural Resources, 2016, Surface geology, 1:100,000—GIS data, November 2016: Washington State Department of Natural Resources Digital Data Series DS-18, version 3.1, previously released June 2010, accessed January 12, 2019, at https://www.dnr.wa.gov/programs-and-services/geology/publications-and-data/gis-data-and-databases.

Wiberg, P.L., and Dungan Smith, J., 1989, Model for calculating bed load transport of sediment: Journal of Hydraulic Engineering, v. 115, no. 1, p. 101–123, accessed September 12, 2020, at https://doi.org/10.1061/(ASCE)0733-9429(1989)115:1(101).

Wolman, M.G., 1954, A method of sampling coarse river-bed material: EOS, Transactions American Geophysical Union, v. 35, no. 6, p. 951–956., accessed February 22, 2022, at https://doi.org/10.1029/TR035i006p00951.

Appendix 1. Inter-Laboratory Comparison of Bedload Sample Processing

Bedload samples collected on December 11 and December 13, 2018, were sent to the U.S. Geological Survey's–Cascades Volcano Observatory (USGS–CVO) sediment laboratory to be sieved and weighed. All subsequent samples were sieved and weighed by the U.S. Geological Survey's–Washington Water Science Center (USGS–WAWSC) sediment laboratory. As a cross laboratory check, four of the composite bedload samples from the December 11, 2018, sampling event initially processed by USGS–CVO laboratory were returned and reprocessed by the USGS–WAWSC laboratory.

Sample processing by the USGS–WAWSC laboratory involved the following steps:

(1). All material coarser than 16 millimeters (mm) was sieved and weighed at full ϕ (16, 32, and 64 mm) intervals. All sieving was done using 300 mm ISO certified sieves; all weights were measured using an Ohaus Range 3000 bench scale, with a 30 kilogram (kg) max weight and 0.001 kg resolution.

(2). Individual coarse clasts were checked with a gravelometer to see if they would be retained on a 128 mm sieve; ultimately, no > 128 mm material was found.

(3). After processing all > 16 mm material, a sample splitter was used to reduce the remaining < 16 mm material into a 3–5 kg split. In cases where the < 16 mm material totaled less than 6 kg, all < 16 mm material was retained. The < 16 mm material was then introduced into a sieve stack with 0.5, 1-, 2-, 4-, and 8-mm sieves and shaken by hand for 2 minutes. Retained material on each sieve was again weighed. Results from the split were then scaled to produce a final estimate of total mass in each size class.

This procedure differs from the USGS–CVO laboratory protocol in two ways; first, USGS–CVO samples were split after sieving to 32 mm, instead of 16 mm; and second, USGS–CVO splits were generally between 1 and 2 kg, instead of 3 to 5 kg.

In terms of total sample mass, USGS–WAWSC laboratory weights for the four reprocessed samples were all less than 1 percent different than USGS–CVO laboratory weights, although USGS–WAWSC weights were consistently lower than USGS–CVO weights (fig. 1.1). In terms of individual full-ϕ bins, USGS-WAWSC weights tended to be lower than USGS–CVO weights through the middle range of size classes (8–64 mm) and higher than USGS–CVO weights across the range of finer material. Although the nominal percentage of difference ranged up to 70 percent, instances of high percentage of error were mostly a product of small sample sizes in the finer size classes; when plotted as cumulative percent finer, results from the two laboratories are comparable (fig. 1.2). Median particle diameters (D_{50}) calculated based on USGS–WAWSC weights differed from those calculated using USGS–CVO weights from -5.1 to 2.4 percent.

The nature of the size-dependent biases between the laboratories also is consistent with a progressive attrition and breakage of clasts due to repeated handling; clasts were observed to be relatively friable. Some of the differences between the laboratories may then be a result of a true change in the grain-size distribution due to repeated handling. However, even if differences were not attributable to attrition, the cross-laboratory differences here are well within acceptable ranges for the purposes of this study.

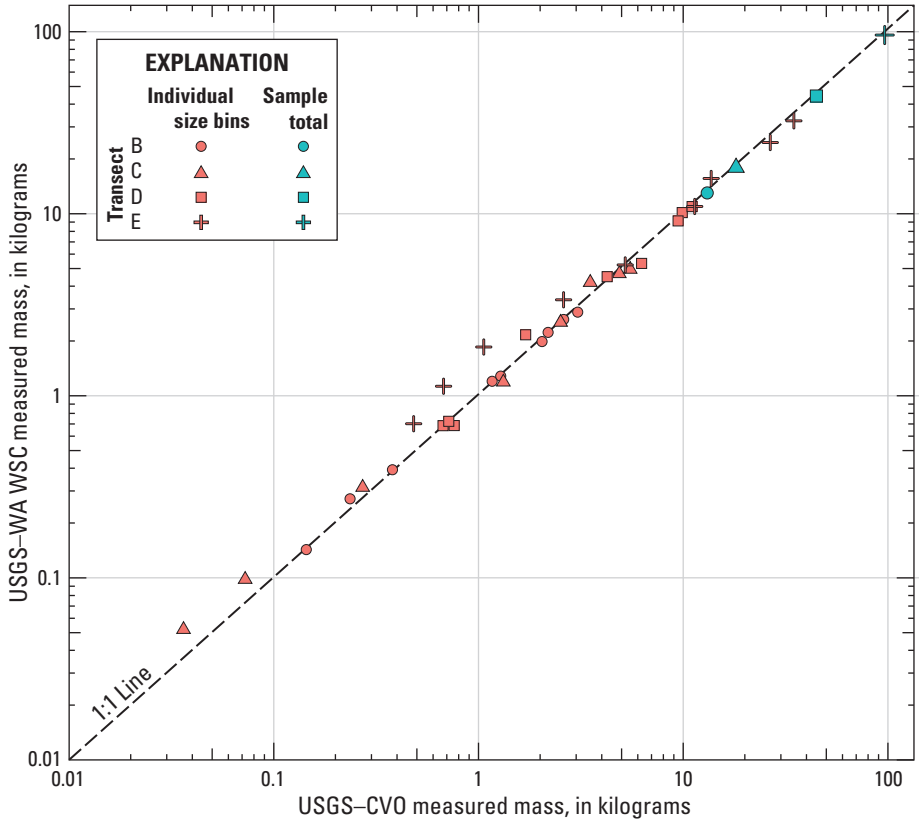

Figure 1.1. Graph showing comparison of bedload sample weights for reprocessed samples.

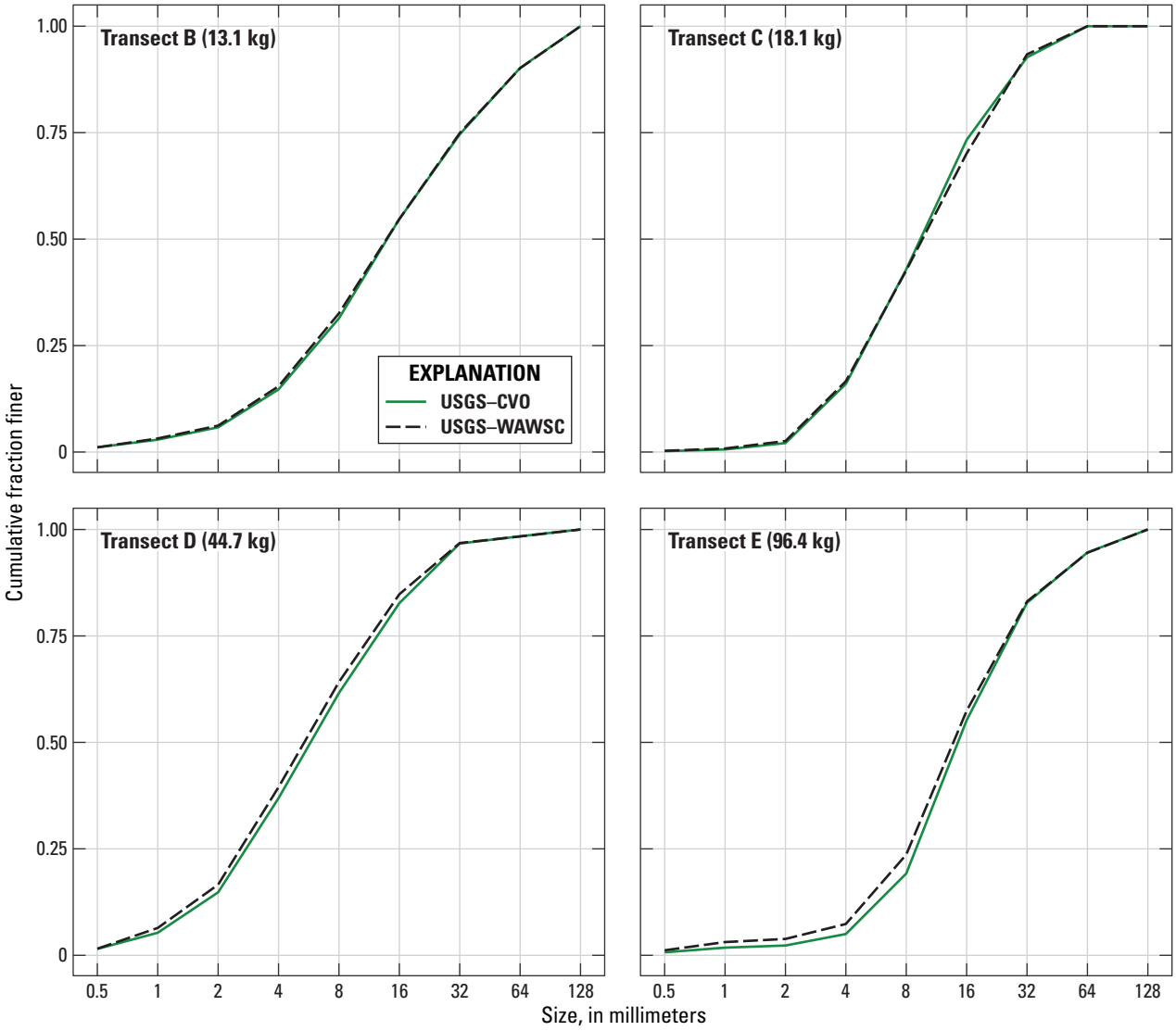

Figure 1.2. Graphs showing comparison of cumulative fraction finer calculated based on results from the U.S. Geological Survey's–Cascade Volcanos Observatory (USGS–CVO) sediment laboratory and re-processing of the same sampled by the U.S. Geological Survey's–Washington Water Science Center (USGS–WAWSC) sediment laboratory.

Appendix 2. Analyses of Sediment Loads and Characteristics at Comparison Sites

The cross-site comparison presented in this study involved some new analyses of available data. Those efforts are detailed here, summarized by site.

Skokomish River

Discharge metrics were based on records at the Skokomish River near Potlatch, Washington (USGS streamgage 12061500), with a period of record from 1943 through the present (2020). Chronic aggradation at the Skokomish River streamgage has made it difficult to maintain accurate stage-discharge ratings for stages greater than 16.55 feet (about 5,000 cubic feet per second [ft^3/s]), and discharges greater than this value have not been published in recent years. To fill these gaps, necessary for characterizing discharge at the site, the discharge at the South Fork Skokomish River, North Fork Skokomish River, and Vance Creek streamgages were summed and compared against published discharge in the main stem. For periods where Vance Creek discharge data were not available, the estimated daily discharge record described in this report was used instead. A linear regression was fit between the "sum of inputs" and the published discharge on the main stem; this linear regression was then used to estimate daily mean discharge in the lower Skokomish River. These estimated values were used to fill days without daily discharge estimates, as well as any day since 2005 with a published discharge greater than 5,000 ft^3/s.

Suspended-sediment and bedload yields for the lower Skokomish River were obtained directly from Collins and others (2019, table 5). Results presented in table 5 were based on analysis methods similar to those used in this study, using bedload and suspended-sediment concentration measurements made by the USGS and Simons and Associates between 1993 and 2010.

Grain-size data for bedload samples were obtained directly from the USGS National Water Information System (NWIS; U.S. Geological Survey, 2020). These data only include bedload samples collected by the USGS. All grain-size distributions collected on a given day were averaged, resulting in five distinct grain-size distributions. These five samples were then averaged to obtain an overall average fraction less than 2 mm (sand fraction), median particle diameter (D_{50}), and 84th percentile particle diameter (D_{84}) for the bedload material.

Elwha River

Discharge metrics for the Elwha River site are based on published discharge at the Elwha River above Lake Mills, Washington (USGS streamgage 12044900), with a period of record from water years 1995 to 1997 and water years 2005 to 2011. This site is in a canyon upstream from the now-removed Glines Canyon Dam.

Suspended-sediment loads were estimated based on application of the suspended-sediment concentration rating curve in Curran and others (2009, fig. 6) to the available discharge record. Bedload measurements collected from 1995 to 1998 were used to construct an unthresholded power law bedload rating curve, which was then used to estimate bedload fluxes over the period of record. Bedload measured at discharges less than 900 ft^3/s were culled from this regression to remove several low-flow measurements that deviated from an otherwise clean log-linear relation with discharge.

Grain-size data for bedload samples are available in Curran and others (2009, appendix C). Sample data were averaged by day to get 23 unique grain-size distributions. Bedload grain-size metrics were calculated as the flux-weighted average of those 23 distributions.

Dungeness River

Discharge metrics for the Dungeness River site were based on discharge records from the Dungeness River at Highway 101 near Sequim, Washington (USGS streamgage 1204800), with a period of record from water years 1923 to 1930 and from water years 1937 to present (2020). Sediment samples were collected at a site about 5 miles downstream (Dungeness River at Highway 101, near Carlsborg, Washington, USGS streamgage 12048600). A comparison among several discharge measurements made at the downstream sediment sampling site and the concurrent 15-minute discharge upstream indicated that, on average, discharge at the downstream site was about 14 percent higher than discharge at the long-term streamgage upstream. The drainage area at the downstream site (178 square miles [mi^2]) also is 14 percent larger than that of the upstream site (156 mi^2). Daily discharge at the upstream site was then uniformly multiplied by 1.14 to obtain a long-term discharge record for the downstream sediment sampling site.

Paired bedload and suspended-sediment load data, including grain-size data for bedload samples, were available through NWIS for the Dungeness River at Highway 101 (USGS streamgage 12048600). The raw sample data were used to construct rating curves using the same basic methods described in the primary report; first, a thresholded power-law regression between sampled bedload and discharge was fit, using a threshold of 500 ft^3/s. That rating curve was then used to estimate bedload at 15-minute intervals over the period of record since water year 2011. The resulting 15-minute record was then summarized to daily results, and a thresholded power law was again used to describe the relation between daily mean discharge and daily total bedload. The same threshold of 500 ft^3/s was used again. That final daily regression was then used to estimate bedload over the full period of available daily discharge records. This same basic process was used to estimate suspended-sediment loads, although using an unthresholded power law as opposed to the thresholded power law. Bedload grain-size data information was obtained as the load-weighted averages of the grain-size distribution of individual bedload samples.

North Fork Skokomish River

Discharge records for the North Fork Skokomish River are based on discharge records for the North Fork Skokomish River below Staircase Rapids, near Hoodsport, Wash. (USGS streamgage 12056500), with a period of record from 1924 to present (2020).

Suspended-sediment concentrations were available at this same site through NWIS; those measurements were used to construct a power-law discharge-SSC rating curve; measurements less than 700 ft^3/s, or where measured SSC was 0, were excluded from the regression. That rating curve was then applied to the available daily discharge records to estimate daily mean SSC and suspended-sediment loads.

References Cited

Collins, B.D., Dickerson-Lange, S.E., Schanz, S., and Harrington, S., 2019, Differentiating the effects of logging, river engineering, and hydropower dams on flooding in the Skokomish River, Washington, USA: Geomorphology, v. 332, p. 138–156., accessed July 11, 2020, at https://doi.org/10.1016/j.geomorph.2019.01.021.

Curran, C.A., Konrad, C.P., Higgins, J.L., and Bryant, M.K., 2009, Estimates of sediment load prior to dam removal in the Elwha River, Clallam County, Washington: U.S. Geological Survey Scientific Investigations Report 2009–5221, 18 p., accessed September 22, 2020, at https://doi.org/10.3133/sir20095221.

U.S. Geological Survey, 2020, USGS water data for the Nation: U.S. Geological Survey National Water Information System database, accessed October 1, 2020, at https://doi.org/10.5066/F7P55KJN.

Publishing support provided by the U.S. Geological Survey
Science Publishing Network, Tacoma Publishing Service Center

For more information concerning the research in this report, contact the
Director, Washington Water Science Center
U.S. Geological Survey
934 Broadway, Suite 300
Tacoma, Washington 98402
https://www.usgs.gov/centers/wa-water

ISSN 2328-0328 (online)
https://doi.org/10.3133/sir20225019